A Technique for Analyzing the Linear Relationships between Two Meteorological Fields

JOHN T. PROHASKA

The Charles Stark Draper Laboratory, Inc., Cambridge Mass. 02139

(Manuscript received 12 April 1976, in revised form 27 August 1976)

ABSTRACT

A method for analyzing the linear relationship field is presented. The empirical orthogonal function technique is utilized directly on the field of time cross-correlation coefficients between two meteorological fields, rather than on the time variation of a spatial meteorological field itself, as in the usual approach. A set of eigenvectors and their corresponding amplitude coefficients is obtained for each eigenvalue. The eigenvector is dependent on the spatial characteristics of the first meteorological field and the amplitude coefficient on the spatial characteristics of the other meteorological field. Because the method maximizes areas of high linear relationship on each of the corresponding grids of the original fields' dominant modes, the areas of significant relationship can be isolated in terms of the explained mean-square correlation.

The technique is illustrated on the zero-lag cross-correlation field between monthly mean Northern Hemisphere sea-level pressure and United States temperature for the midseason months of January, April, July and October during the 59-year period from 1912 to 1970.

1. Introduction

In the course of investigating the selection of analogs for long-range prediction of United States monthly mean temperatures by Northern Hemisphere sea-level pressure anomaly patterns, the need for a method of isolating important predictive elements and reducing the amount of material to be examined becomes apparent. The method of empirical orthogonal functions has been applied to time series of meteorological data (Kutzbach, 1967; Lorenz, 1956) for similar purposes. However, here our interest is not in the time variation and patterning of the temperature or pressure fields, but in the patterning of the pressure-temperature correlation coefficient field.

To this purpose, an empirical orthogonal function technique for analyzing the linear correlation field, which is obtained from the time correlation of two meteorological fields, is presented. This method affords an opportunity to isolate the corresponding highly related areas of the two original meteorological fields, and to reduce significantly the degrees of freedom of the linear relationship field. The eigenvectors and the corresponding amplitude coefficients are to be computed from the solution of the eigenvalue problem for the mean-product matrix of the cross correlations. The mean product, rather than the covariance, is of interest because information about the distribution of the total amount of correlation, rather than the variation about the mean correlation, is desired. We will refer to these statistics as the mean-square correlation, the mean product and explanation of the mean-square correlation by analogy with the terms variance, covariance and reduction of variance—commonly used in the application of the method of empirical orthogonal functions.

Canonical correlation has been applied to pairs of fields in order to maximize the correlation between the linear combinations of predictors and predictands. Sets of weighting coefficients for the predictors and predictands are simultaneously obtained, and are associated with particular eigenvalues representing the multiple correlation between the fields (Glahn, 1968). The linear combinations of predictors are optimal predictors of the linear combinations of predictands. By comparison the analysis presented in this paper is more diagnostic than predictive. The cross correlations of each predictor with all other predictands are examined by obtaining the principal components, thereby obtaining a partitioning of the correlation field into a representation on the predictor grid and a paired representation on the predictand grid for each mode. The eigenvalues, in this case, are the mean-square correlations between the predictor and predictand fields for each mode. This method is more useful for examining the nature of the linear relationships between the predictor and predictand fields, as they actually exist, than for obtaining a linear prediction.

An illustration of the technique, the linear correlation field at zero lag between the fields of monthly mean Northern Hemisphere sea-level pressure and tempera-

TABLE 1. Temperature grid stations.

1. Portland, Me.	17. Knoxville, Tenn.
2. Buffalo, N. Y.	18. Cairo, Ill.
3. Sault Ste Marie, Mich.	19. Wichita, Kans.
4. Minneapolis, Minn.	20. Pueblo, Colo.
5. Williston, N. D.	21. San Francisco, Calif.
6. Helena, Mont.	22. Los Angeles, Calif.
7. Victoria, B. C.	23. Flagstaff, Ariz.
8. Medford, Ore.	24. El Paso, Tex.
9. Winnemucca, Nev.	25. Abilene, Tex.
10. Salt Lake City, Utah	26. Corpus Christi, Tex.
11. Rapid City, S. D.	27. Shrevesport, La.
12. Omaha, Nebr.	28. Mobile, Ala.
13. Chicago, Ill.	29. Savannah, Ga.
14. Parkersburg, W. Va.	30. Tampa, Fla.
15. Atlantic City, N. J.	31. Halifax, N. S.
16. Cape Hatteras, N. C.	32. Ottawa, Ont.

ture at stations in the United States and Canada, is examined.

2. Data

The method of analysis described is demonstrated by decomposing the zero-lag correlation coefficient field obtained from monthly mean temperatures and sea-level pressures. Fifty-nine years of data from 1912 to 1970 are available for the midseason months of January, April, July and October. The sea-level pressure grid consists of 181 approximately equally spaced grid points on the Northern Hemisphere from 20°N to the pole. The grid interval is 10° longitude at 20, 30, 40 and 50°N. At 60°N, an interval of 20° longitude is used, and the interval is expanded to 40° longitude at 70° and 80°N. Finally, the pole point completes the grid. The temperature data are from 32 United States and Canadian stations (Table 1). These temperature stations are also approximately evenly spaced. Both the mean temperature and sea-level pressure data are climatological records from a period of generally reliable data.

3. Method of analysis

The temperature field is denoted by T_{st}, where $s=1$ to 32 stations and $t=1$ to 59 for the years 1912 to 1970 for each of four midseason months. The sea-level pressure field is denoted by P_{gt}, where $g=1$ to 181 Northern Hemisphere grid points and $t=1$ to 59 for the same years and for the corresponding midseason months. The specification of the temperature field by the concurrent pressure field is the relationship of interest.

Further we define $T'_{st}=(T_{st}-\overline{T_s})/S_s$ and $P'_{gt}=(P_{gt}-\overline{P_g})/S_g$, where $\overline{T_s}$ and $\overline{P_g}$ are the means and S_s and S_g sample standard deviations calculated over 59 years of data. Then the (32 by 181) cross-correlation coefficient matrix $(\mathbf{C}_{sg})$

$$\mathbf{C}_{sg}=\left(\sum_{t=1}^{59} T'_{st}*P'_{gt}\right)/59 \tag{1}$$

is computed between each of the standardized time series of temperature at the 32 stations and those of sea-level pressure at the 181 grid points at zero lag.

The (32 by 32) mean-product matrix

$$\mathbf{H}_{s1s2}=\left(\sum_{g=1}^{181} \mathbf{C}_{s1g}*\mathbf{C}_{s2g}\right)/181 \tag{2}$$

for

$$s1,\ s2=1 \text{ to } 32$$

is calculated, where the product of the correlation coefficients at each pressure grid point for each temperature station ($s1$) with all other temperature stations ($s2$) is averaged over the 181 pressure grid points.

Now the matrix equation

$$(\mathbf{H}-\lambda\mathbf{I})\mathbf{U}=0 \tag{3}$$

can be solved for the set of 32 orthonormal eigenvectors $(\mathbf{U}_{si})$ and eigenvalues (λ_i), where $i=1$ to 32 functions in order of decreasing explained mean-square correlation (Lorenz, 1956). With the eigenvectors $(\mathbf{U}_{si})$ and the original correlation matrix $(\mathbf{C}_{sg})$, an amplitude coefficient matrix can be defined by the relationship

$$\mathbf{Q}_{ig}=\sum_{s=1}^{32} \mathbf{C}_{sg}*\mathbf{U}_{si} \tag{4}$$

so that the original correlation coefficient matrix

$$\mathbf{C}_{sg}=\sum_{i=1}^{32} \mathbf{Q}_{ig}*\mathbf{U}_{si} \tag{5}$$

can be reconstructed by a linear combination of the amplitude coefficients and eigenvectors. The coefficients are dependent only on pressure grid point, and the eigenvectors are dependent only on temperature station. The correlation coefficient patterns are partitioned into pairs of patterns: one pattern displaying the contribution of the pressure field to the correlation coefficient and the other pattern displaying the contribution of the temperature field. The pair of patterns corresponding to the largest eigenvalue contributes the largest portion of the mean-square correlation considered over all pressure grid points and temperature stations. There is a corresponding decreasing contribution to the mean-square correlation for the smaller eigenvalues. Where the explanation of the mean-square correlation coefficient can be accomplished with relatively few functions, a limited set of modes dominates the relationship between the pressure and temperature fields. When, for any function, the independent contribution to the correlation coefficient between a temperature station and pressure grid point is computed, the sign and magnitude of the correlation coefficient is determined by the product.

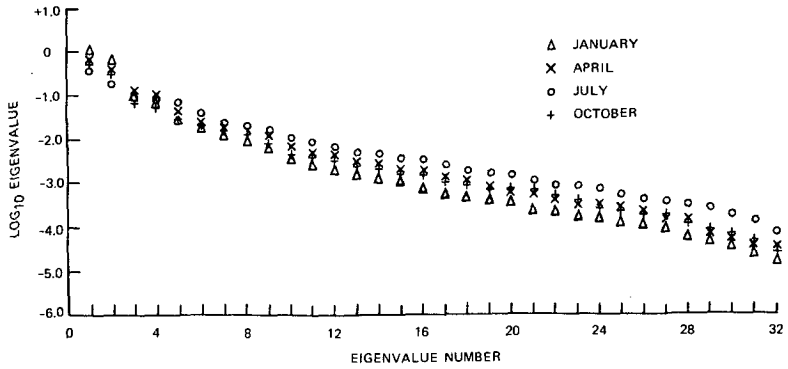

FIG. 1. LEV diagram—logarithm of the eigenvalue versus the eigenvector number for the cross-correlation coefficients of Northern Hemisphere sea-level pressure against temperature over the United States for the midseason months of January, April, July and October.

From the orthonormal properties of the eigenvectors, it follows that, for any i

$$\sum_{s1,s2} \mathbf{U}_{s1i}*\mathbf{U}_{s2i}=\begin{cases}0, & \text{for } s1\neq s2\\ 1, & \text{for } s1=s2.\end{cases} \tag{6}$$

Now from (3), (5) and (6) we can obtain an expression for the eigenvalues

$$\lambda_i=(\sum_{g=1}^{181} Q_{ig}^2)/181 \tag{7}$$

so that the magnitude of the mean-square correlation coefficient is contained in the square of the amplitude coefficients (Q_{ig}) averaged over the 181 grid points.

From (5), (6) and (7), an expression for the root-mean-square (rms) correlation coefficient can be obtained:

$$(\overline{\mathbf{C}_{sg}^2})^{\frac{1}{2}}=[(\sum_{i=1}^{32}\lambda_i)/32]^{\frac{1}{2}}. \tag{8}$$

From (8), it can be seen that the magnitude of the rms correlation is described solely by the set of eigenvalues (λ_i).

4. Discussion of statistical results

An examination of the statistical results of the analysis of the pressure-temperature relationship field demonstrates a number of interesting points. Relatively few dominant modes explain a large portion of the mean-square correlation coefficient, and the eigenvector (U) and amplitude coefficient (Q) patterns deviate appreciably from randomness for the larger eigenvalues. There is also a marked seasonal variation in the linear relationship between pressure and temperature fields with a maximum relationship in January and a minimum in July.

A technique for determining which eigenvectors deviate appreciably from randomness is desirable. Following the analysis of Farmer (1971), and Craddock and Colgate (1974), a log eigenvalue versus eigenvector number (LEV) diagram was plotted (Fig. 1), for the four midseason months. The characteristics of this LEV diagram generally followed the pattern observed by Farmer (1971). The log eigenvalues corresponding to the first third of the eigenvector numbers deviate considerably from the straight line fitted to the essentially random last two-thirds of the eigenvector numbers. Farmer has shown that a LEV diagram of random data is linear, and that there is a sharp tail off from linearity for the last few eigenvector numbers. This deviation is attributed to the scale of the patterns being smaller than the grid spacings, and to a loss of degrees of freedom (Craddock and Colgate, 1974). Certainly, the first few functions can be considered nonrandom.

The January curve has the greatest deviation from the straight line denoting randomness. The equinoctial months' curves deviate about equally and lie between

TABLE 2. Percent explanation of the mean-square correlation coefficient.

Individual functions				
Functions	January	April	July	October
1	58.1	40.7	40.0	47.3
2	28.5	31.5	18.0	30.3
3	5.4	9.7	11.2	7.1
4	3.4	6.7	8.3	5.0
5	1.5	3.3	7.3	2.9
6	1.0	2.1	3.5	1.9
Cumulative functions				
Functions	January	April	July	October
1 to 2	86.6	72.2	58.0	77.6
1 to 3	92.0	81.9	69.2	84.7
1 to 4	95.4	88.6	77.5	89.7
1 to 5	96.9	91.9	84.8	92.6
1 to 6	97.9	94.0	88.3	94.5

the January and July curves. For the larger eigenvalues, the July curve deviates least from the randomness described by the straightline relationship of the LEV diagram.

An inspection of Table 2 shows a rather sizable explanation of the mean-square correlation coefficient field by the first six functions for all four midseason months. The largest explanation of 97.9% for the first six functions occurs in January with a low of 88.3% for July. April and October have explanations of the mean-square correlation of 94.0 and 94.5%, respectively, lying between the summer and winter month values.

The first two functions for each midseason month define the two dominant modes, by which the relationship between the United States temperature field and the Northern Hemisphere sea-level pressure field can, in large part, be described. These two functions describe the largest scale patterns and a large portion of their respective month's mean-square correlation, that is, 86.6, 72.2, 58.0 and 77.6% for January, April, July and October, respectively. The cross-correlation field between temperature and pressure sets up in a rather limited number of modes, which are clearly related to the centers of action of the general circulation. An inspection of higher order modes shows a decrease in the scale and an increase in the complexity of the patterns as the randomness increases.

In order to establish a reference level for the correlation coefficient, we arbitrarily select the 5% level commonly used in statistical analysis. There are 59 pairs of temperature and pressure values in the computation of each correlation coefficient, the distribution of random correlation coefficients has a mean of zero, and its standard deviation can be approximated by $(1/59)^{\frac{1}{2}}$, or 0.13. By choosing the Students' t value at the 5% level for 57 degrees of freedom or ($t=2.00$), we can obtain the value (0.26) of the correlation coefficient at the 5% level. The statement can now be made that at the error risk of 1 chance in 20, a correlation coefficient exceeding 0.26 will differ from the correlation of zero, denoting a random relation.

From (8) an rms correlation coefficient for each station and grid point pair can be computed. Again, it is seen that there is a seasonal trend from a high correlation of 0.240 in January to a low of 0.175 in July with mid-range values of 0.204 and 0.185 for April and October, respectively. With correlations of these magnitudes (correlations which are averaged over all grid point and station pairs), it is reasonable to expect high correlations in areas of limited extent.

In order to interpret the patterns of relationship between the temperature and pressure fields, it is useful to demark the more statistically significant corresponding areas of the 32 temperature-station eigenvector patterns and the 181 pressure grid-point amplitude coefficient patterns. Since the product of the amplitude coefficient (Q) and the eigenvector (U) equals the contribution to the correlation coefficient for any particular mode, then for any given level of correlation coefficient, boundary values on the Q field and U field may be adjusted to balance the size of the encircled areas on each of the fields. Arbitrarily selecting the 5% significance level correlation coefficient of 0.26, two sets of boundaries are established on the Q field and U field. The first set matched the value 0.245 on the U field with 1.06 on the Q field, while the boundary value 0.145 on the U field was paired with a value of 1.79 on the Q field for the second set. Each of these pairs of eigenvector and amplitude coefficient values demarks areas of correlation contribution, which exceed the 5% significance level. Clearly, the smaller the boundary value is, the larger the area enclosed. Thus, an increased area on the Q field is matched by a decreased area on the U field and vice versa. The first boundary pair is selected to show more clearly the extent of the pattern on the Q field, while the second pair is for the clarification of the U field patterns. Because the patterns of two fields are referred to by pairs, it is necessary to distinguish the isopleths by differing boundary designations. Added isopleths would require different distinguishing boundary designations, resulting in increased confusion for the reader.

In Table 3, the counts of the number of points for the 32 stations and 181 grid points equaling or exceeding the 0.245 and 1.06 limits are displayed for the dominant modes of the first and second functions.

No attempt is made here to judge the significance of the counts by a comparison with the expectation at the 5% level because of the high degree of interdependence between the points within each of the fields. Again the seasonal variation is seen with a maximum in the counts for January and a minimum for July. Also, there is an expected decrease in the counts from the first mode to the second mode. It could be expected that the other modes (with their rapidly decreasing explanation of the mean-square correlation) would have proportionately lower counts of points contributing to significant correlations than the modes having large eigenvalues.

5. Synoptic discussion

The synoptic discussion deals with the interpretation of the pressure-temperature specification relationships in the form of amplitude coefficient patterns on the Northern Hemisphere grid and the corresponding

TABLE 3. Counts of points $\geq$ 5% level for 181 grid-point Q field of pressure and 32 station U field of temperature.

		January	April	July	October
Mode 1	U field	7	5	5	6
	Q field	69	26	21	22
Mode 2	U field	8	7	4	6
	Q field	26	18	0	13

eigenvector patterns over the United States. The amplitude coefficient patterns, referred to here as the Q field patterns, are superposed upon the mean monthly long-term (1899–1967) sea-level pressure (dash line) patterns. The eigenvector patterns on the United States station temperature grid are referred to as the U field patterns. The amplitude coefficients (Q) are displayed in Figs. 2a–8a and the corresponding eigenvectors (U) in Figs. 2b–8b, respectively.

In the interpretation of the synoptic patterns, two points should be borne in mind:

1) The correlation coefficient has the magnitude and sign of the product of the values at a grid point of the Q field and at a station of the U field.

2) Since the correlation coefficient is a measure of the linear relationship, for any given correlation an extreme positive pressure anomaly corresponds with an appropriate extreme temperature anomaly and there is an opposite extreme temperature anomaly corresponding to a negative pressure anomaly.

In the following synoptic discussions, the signs of the correlation coefficients between significant areas on the Q field and U field are determined from the product of the selected amplitude coefficient and eigenvector. A pressure anomaly is assumed in the Q field region under consideration, and the temperature anomaly in the corresponding U field region is linearly estimated. A reversal of that pressure anomaly sign, of course, is followed by a reversal of the temperature anomaly sign.

a. January—Mode I (58.1% of mean-square correlation)

There are three large cells shown in Fig. 2a in which pressure correlates significantly with temperature in the southeastern United States (Fig. 2b). This correlation is positive with the Pacific and Atlantic cells and negative with the North American cell. High January temperatures in the southeast United States are associated with a rise in pressure in the Aleutian low with an expansion of the eastern Pacific high-pressure cell north and westward, and an expansion of the Atlantic subtropical high-pressure belt northerly toward the Icelandic low and easterly toward the Siberian high through central Europe. Over central North America, there is a decrease in the normally high January pressure as the Icelandic low deepens and expands westward over the Canadian Arctic and Greenland.

This pressure pattern gives rise to colder temperatures over California, but the correlation is lower than with the southeastern United States temperature.

Conversely, a cold eastern United States and a warm West Coast occurs with a deepening of the Aleutian low and its expansion southeasterly into the eastern cell of Pacific subtropical high pressure. The pressure rises over the central United States and Canada and into the Arctic expanding over Greenland with the Icelandic low filling in its normal position. The Icelandic low is pushed south over the region of the Azores high and southeasterly over the western Atlantic.

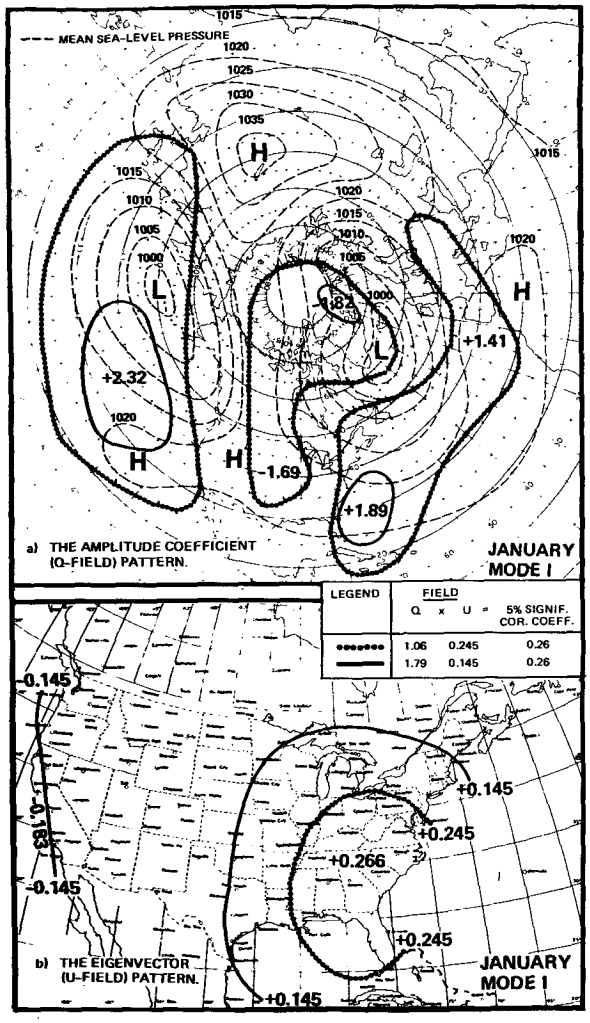

FIG. 2. Patterns for January Mode I explaining 58.1% of the mean-square correlation coefficient.

The pressure pattern corresponding to a cold eastern United States is strongly meridional with strong pressure gradients. The pressure gradients are considerably weaker with warm temperatures in the same area.

b. January—Mode II (28.5% of mean-square correlation)

Two correlation cells are present on the pressure grid (Fig. 3a). One cell occurs at 20°N in the eastern Pacific, the other is an east-west band from the Gulf of Alaska across Canada and the northern United States into the western Atlantic. The large cell has a negative correlation with an area over the northwestern United States into the Central Plains, and a positive correlation with Florida (Fig. 3b). The correlations are opposite for the lower latitude Pacific cell.

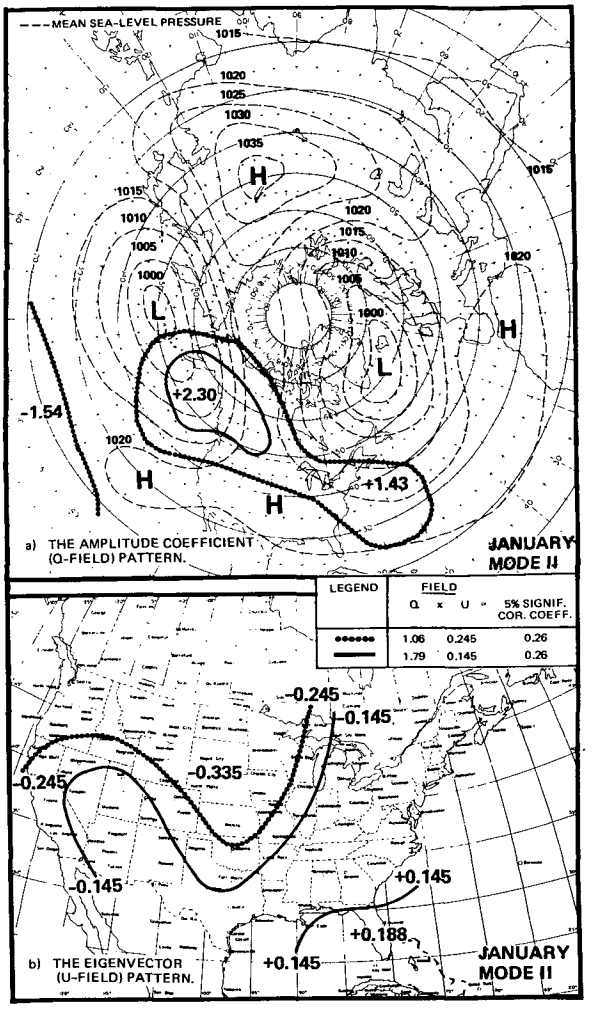

FIG. 3. Patterns for January Mode II explaining 28.5% of the mean-square correlation coefficient.

Low temperatures over the Plains and Pacific Northwest and high temperatures over Florida occur with an increase in pressure over the Gulf of Alaska and off the East Coast. The pressure in the Canadian high increases and pressure in the low-latitude (20°N) Pacific decreases, resulting in a decrease in the westerlies on the West Coast. The increase in pressure off the East Coast increases a southeasterly flow over Florida.

High temperatures in the Northwest and over the Central Plains, and cold temperatures over Florida are accompanied by a decrease of pressure off the East Coast with an increased flow from the northwest over Florida. An expansion of the Aleutian low eastward and a decrease in pressure of the Canadian high, along with an increase in pressure in the Pacific subtropical high pressure, results in increased zonal westerlies and warmer temperatures in the Northwest and into the Plains.

c. April—Mode I (40.7% of mean-square correlation)

The eigenvector U field pattern consists of a positive cell centered over the lower Great Lakes and Ohio River valley with an opposite signed cell over California (Fig. 4b). The corresponding Q field pattern has seven cells, each associated with some major feature of the normal pressure pattern (Fig. 4a).

High temperatures in the eastern United States and concurrent low temperatures over the West Coast are accompanied by a deepening of the thermal low over the Western Plains from Canada to Mexico and an expansion of the subtropical Pacific high toward the Aleutian low from the southeast and from the southwest over Japan. There is also an increase in pressure over the St. Lawrence River and Central Europe on the southwest and southeast extensions, respectively, of the Icelandic low. The Azores high experiences a decreased pressure on its southerly edge. Over the South China Sea, the thermal low centered over India is bounded by rising pressure. In general, with the move-

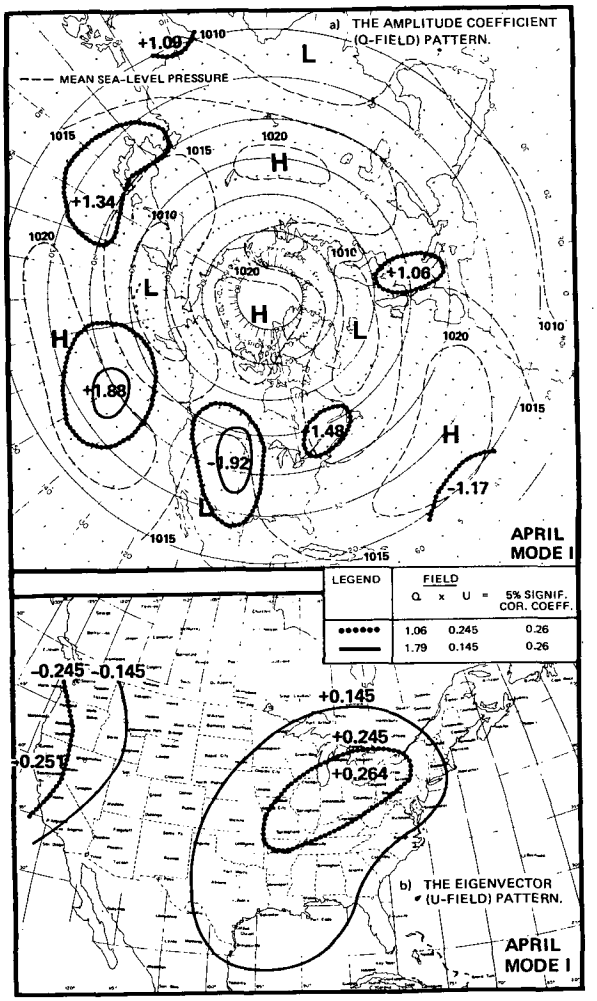

FIG. 4. Patterns for April Mode I explaining 40.7% of the mean-square correlation coefficient.

ment of subtropical highs northward over the oceans into the regions of the oceanic lows and a decrease in pressure over North America, there is an increased meridional circulation with an anomalous southerly wind field in the eastern United States, and a northerly flow over the West Coast.

The reversed pattern of a warm West Coast and cold in the central states results from increased zonal westerlies off the Pacific and a decrease in the southwesterly or a turn to a northeasterly flow out the Hudson Bay region. The general circulation from the Pacific to the Atlantic becomes more zonal.

d. April—Mode II (31.5% of mean-square correlation)

The correlation pattern consists of a single cell out of Canada from the western Great Lakes west to the Pacific, and south over the Plateau into Nevada and Utah on the *U*-field (Fig. 5b). The *Q* field has four cells (Fig. 5a). One cell on the eastern edge of the thermal low is centered over Louisiana. It is related to the expansion or contraction of the thermal low eastward into the Mississippi Valley. The other three cells are, respectively, on the eastern end of the Pacific subtropical high-pressure cell, the second related to the Arctic high-pressure cell, and the last to the interaction of the Icelandic low and the Azores high.

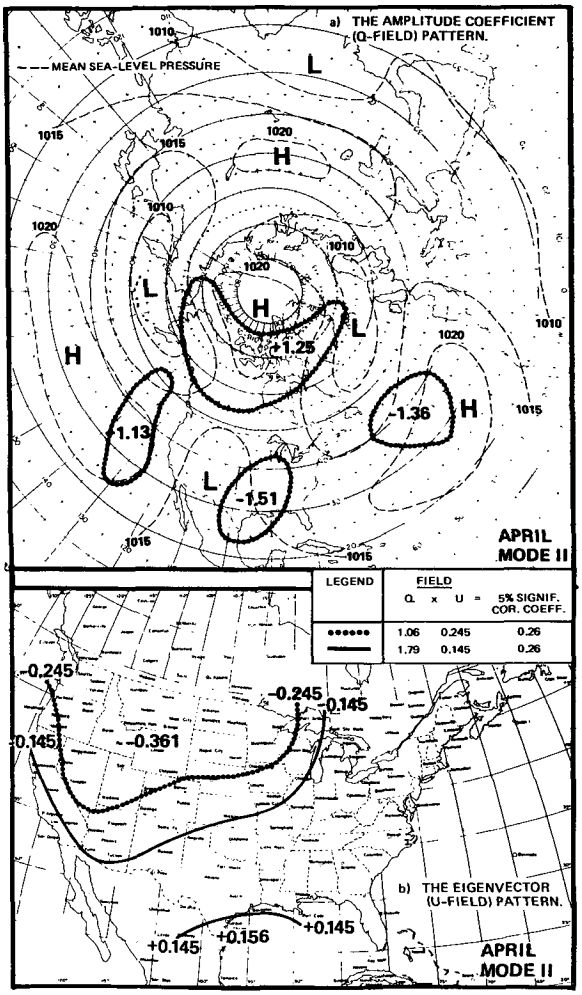

FIG. 5. Patterns for April Mode II explaining 31.5% of the mean-square correlation coefficient.

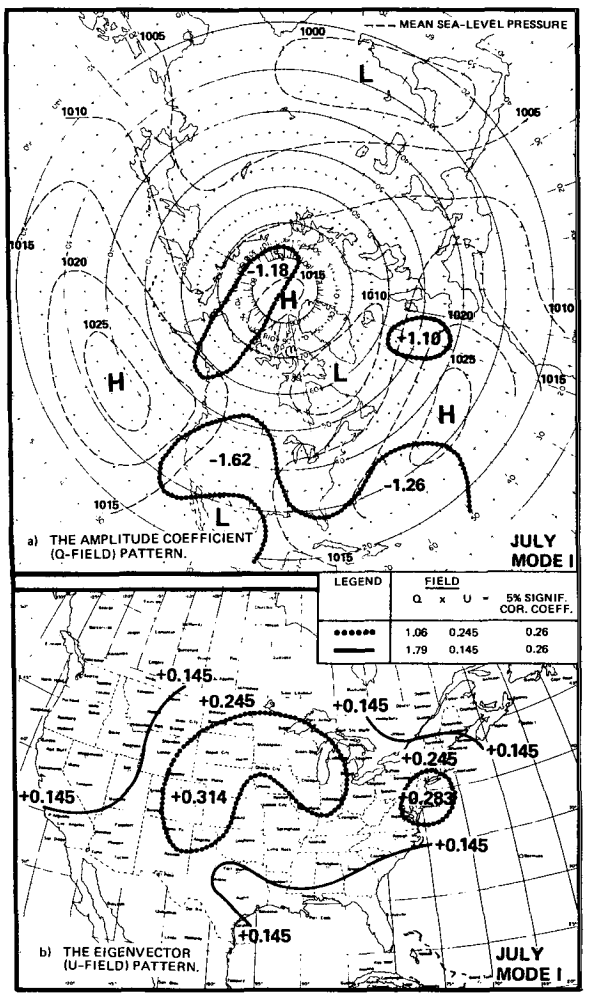

FIG. 6. Patterns for July Mode I explaining 40.0% of the mean-square correlation coefficient.

Low temperatures in the *U* field cell centered over Montana accompanies an expansion of the Arctic high pressure southward over Canada and in an east-west direction into the northern fringes of both the Icelandic and Aleutian lows, an enlarged thermal low over the Mississippi Valley, an increase in pressure off the West Coast and an expansion of the Icelandic low into the central North Atlantic. A ridge of high pressure grows over the eastern Pacific into the Canadian Arctic with troughing in the United States east of the Rockies and into the Icelandic low.

The reverse pattern of warm temperatures occurs with a more zonal circulation in the eastern Pacific,

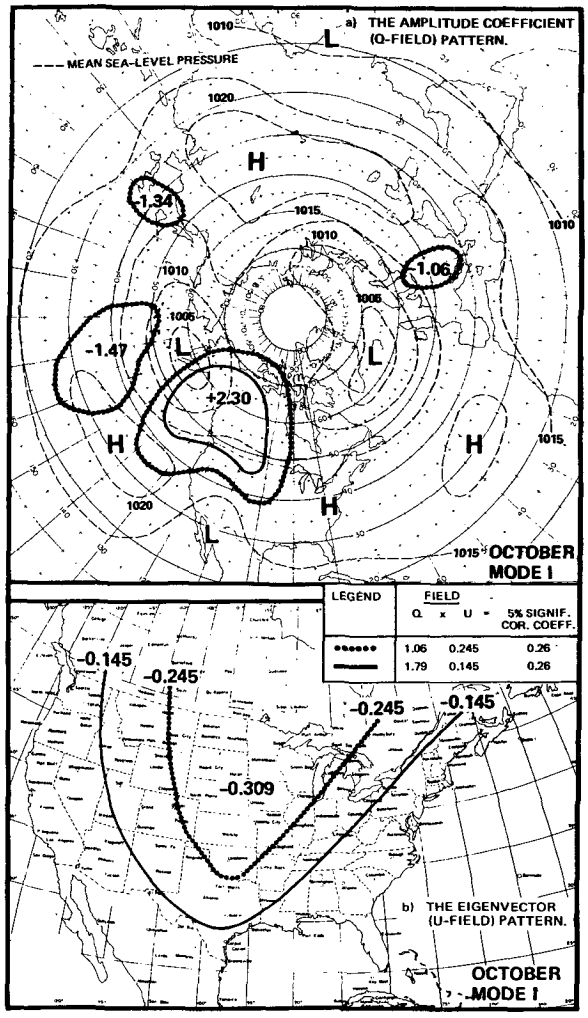

FIG. 7. Patterns for October Mode I explaining 47.3% of the mean-square correlation coefficient.

an enhancement of the circumpolar low-pressure vortex, ridging over the eastern United States, and an expansion of the Azores high northward.

e. July—Mode I (40.0% of mean-square correlation)

The temperature correlation component on the U field has two cells. A small cell is located over New Jersey and a large one extends from the Rockies east to the Great Lakes (Fig. 6b). The Q field has essentially four cells. One is related to the Arctic high pressure, two are associated with northeast-southwest shift of the Atlantic high-pressure cell (Fig. 6a). Probably the most important to the temperature pattern is the cell over the thermal low-pressure area in the western United States.

Warm temperatures in the central United States result from the increased southwesterly winds generated by the deepening thermal low. Simultaneously, there is a northeasterly shift of the Azores high and a decrease in the Arctic high pressure.

A reversal to cold temperatures in the affected parts of the United States is accompanied by anomalously high pressure in the United States and a high-latitude zonal circulation with westerly and northwesterly circulation in the central and eastern United States.

f. October—Mode I (47.3% of mean-square correlation)

The U field pattern consists of a large wedge extending out of Canada into the Plains from the Rockies east to the Appalachians and south to Mexico and the Gulf of Mexico (Fig. 7b). On the corresponding pattern of the Q field are two major cells associated with the shifting of the Aleutian low and the eastern Pacific subtropical high (Fig. 7a). Two other small cells, one to the southwest of the Aleutian low and the other to the southeast of Icelandic low, are probably relatively unimportant.

The U field pattern is negatively correlated with the large cell on the eastern edge of the Aleutian low over western Canada, Alaska and the Gulf of Alaska, and

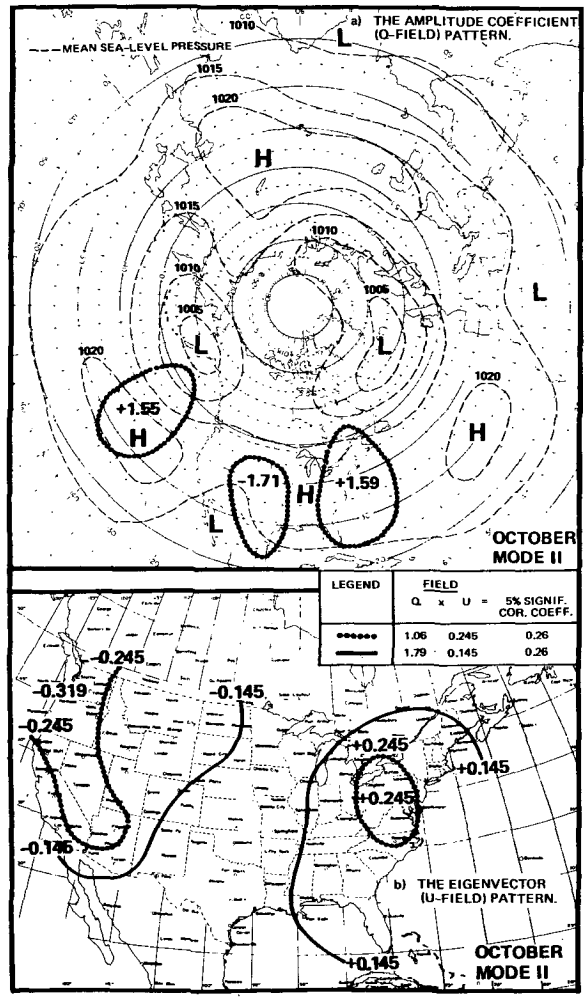

FIG. 8. Patterns for October Mode II explaining 30.3% of the mean-square correlation coefficient.

positively correlated with the cell to the south of the Aleutian low and to the northwest of the Pacific high.

An anomalous cold wedge over the Plains is associated with a shift of the Aleutian low westward and southward into the western portions of the subtropical high and a ridging over western Canada with an attendant northwesterly flow into the Plains. The two minor cells imply a movement of the western edge of the Aleutian low over Japan and the southeastern edge of the Icelandic low over central Europe.

Anomalous warmth in the Plains states is related to a movement of the Aleutian low and the trough position eastward, bringing a more westerly wind flow into the central United States.

g. October—Mode II (30.3% of mean square correlation)

The U field pattern consists of two cells of opposite sign, one over the eastern and the other over the western United States (Fig. 8b). The corresponding Q field pattern is dominated by three cells. The Q field cell over the central United States is negatively correlated with the western U field cell (Fig. 8a). The other two Q field cells, having positive correlations with the U field cells in the eastern and negative correlations in the western United States, are located over the East Coast and offshore on the West Coast. A pattern of cold temperatures in the West and warm temperatures in the East occurs with a ridging in the Pacific high-pressure cell, a deepening of the thermal low in the Southwest and a ridging in the Bermuda high over the East Coast, resulting in a northwest wind over the West Coast and a southwest wind component over the East Coast.

Conversely, a cold temperature in the East and warm in the West occurs with a relative troughing in the Western Atlantic and in the Pacific off the West Coast and an anomalous ridging over the Central Plains. This pattern reflects a reversal of the wind field.

6. Conclusions

Clearly, the technique presented offers a way of determining the relative contribution of two meteorological fields to their common field of linear relationship. The spatial distribution of the contributions by the fields of the eigenvectors and amplitude coefficients are coherent and, for the example, are consistent with the mean patterns of temperature anomalies over much of North America. The technique also results in a rather extensive reduction in the number of synoptic patterns of relationship, so that the essential features of the relationship field are isolated into relatively few dominant modes.

In the example illustrated, a zero-lag field of correlation coefficients between the elements of two meteorological fields is examined. The technique, of course, can be applied to any pair of fields, such that the dimensions of the resulting cross-correlation field can be reasonably coped with in the eigenanalysis. Also, there is no restriction to zero-lag correlations; and lag correlation fields may be examined at any practically useful lag.

Because the method is effective in isolating the geographic regions of high linear relationship, it can be useful in the matching of moderate size anomalies to the large-scale features of the planetary patterns for the selection of analogs for long-range prediction. For direct statistical prediction at selected time lag, the method provides an ability to screen out areas of less linearly related predictors and to reduce the chance of including spurious predictors.

Acknowledgments. The author expresses his appreciation to Dr. Hurd C. Willett, Dr. Edward N. Lorenz, Dr. Reginald E. Newell and Dr. Brian C. Weare of the MIT Meteorology Department for their critical comments.

REFERENCES

Craddock, J. M., and M. G. Colgate, 1974: The use of eigenvectors for smoothing and prediction. *Bull. Inst. Math. Appl.*, **10**, 152–160.

Farmer, S. A., 1971: An investigation of the results of principal component analyses of data derived from random numbers. *The Statistician*, **20**, 63–72.

Glahn, H. R., 1968: Canonical correlation and its relationship to discriminant analysis and multiple regression. *J. Atmos. Sci.*, **25**, 23–31.

Kutzbach, J. E., 1967: Empirical eigenvectors of sea-level pressure, surface temperature and precipitation complexes over North America. *J. Appl. Meteor.*, **6**, 791–802.

Lorenz, E. N., 1956: Empirical orthogonal functions and statistical weather prediction. Sci. Rep. No. 1, Statistical Forecasting Project, Dept. Meteor., M.I.T., 49 pp.